Molecular spectroscopy 2: electronic transitions

14

Simple analytical expressions for the electronic energy levels of molecules cannot be given, so this chapter concentrates on the qualitative features of electronic transitions. A common theme throughout the chapter is that electronic transitions occur within a stationary nuclear framework. We pay particular attention to spontaneous radiative decay processes, which include fluorescence and phosphorescence. A specially important example of stimulated radiative decay is that responsible for the action of lasers, and we see how this stimulated emission may be achieved and employed.

The energies needed to change the electron distributions of molecules are of the order of several electronvolts (1 eV is equivalent to about 8000 cm^{-1} or 100 kJ mol^{-1}). Consequently, the photons emitted or absorbed when such changes occur lie in the visible and ultraviolet regions of the spectrum (Table 14.1).

One of the revolutions that has occurred in physical chemistry in recent years is the application of lasers to spectroscopy and kinetics. Lasers have brought unprecedented precision to spectroscopy, made Raman spectroscopy a widely useful technique, and have made it possible to study chemical reactions on a femtosecond time scale. We shall see the principles of their action in this chapter and their applications throughout the rest of the book.

The characteristics of electronic transitions

In the ground state of a molecule the nuclei are at equilibrium in the sense that they experience no net force from the electrons and other nuclei in the molecule. Immediately after an electronic transition they are subjected to different forces and

Synoptic table 14.1* Colour, frequency, and energy of light

Colour	λ/nm	ν/(10^{14} Hz)	E/(kJ mol^{-1})
Infrared	>1000	<3.0	<120
Red	700	4.3	170
Yellow	580	5.2	210
Blue	470	6.4	250
Ultraviolet	<300	>10	>400

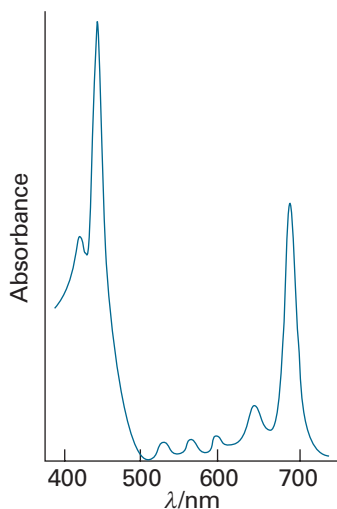* More values are given in the *Data section*.

Fig. 14.1 The absorption spectrum of chlorophyll in the visible region. Note that it absorbs in the red and blue regions, and that green light is not absorbed.

Comment 14.1

It is important to distinguish between the (upright) term symbol Σ and the (sloping) quantum number Σ.

the molecule may respond by starting to vibrate. The resulting vibrational structure of electronic transitions can be resolved for gaseous samples, but in a liquid or solid the lines usually merge together and result in a broad, almost featureless band (Fig. 14.1). Superimposed on the vibrational transitions that accompany the electronic transition of a molecule in the gas phase is an additional branch structure that arises from rotational transitions. The electronic spectra of gaseous samples are therefore very complicated but rich in information.

14.1 The electronic spectra of diatomic molecules

We examine some general features of electronic transitions by using diatomic molecules as examples. We begin by assigning term symbols to ground and excited electronic states. Then we use the symmetry designations to formulate selection rules. Finally, we examine the origin of vibrational structure in electronic spectra.

(a) Term symbols

The term symbols of linear molecules (the analogues of the symbols ^2P, etc. for atoms) are constructed in a similar way to those for atoms, but now we must pay attention to the component of total orbital angular momentum about the internuclear axis, $\Lambda\hbar$. The value of $|\Lambda|$ is denoted by the symbols $\Sigma, \Pi, \Delta, \ldots$ for $|\Lambda| = 0, 1, 2 \ldots$, respectively. These labels are the analogues of S, P, D, $\ldots$ for atoms. The value of Λ is the sum of the values of λ, the quantum number for the component $\lambda\hbar$ of orbital angular momentum of an individual electron around the internuclear axis. A single electron in a σ orbital has $\lambda = 0$: the orbital is cylindrically symmetrical and has no angular nodes when viewed along the internuclear axis. Therefore, if that is the only electron present, $\Lambda = 0$. The term symbol for H_2^+ is therefore Σ.

As in atoms, we use a superscript with the value of $2S + 1$ to denote the multiplicity of the term. The component of total spin angular momentum about the internuclear axis is denoted Σ, where $\Sigma = S, S - 1, S - 2, \ldots, -S$. For H_2^+, because there is only one electron, $S = s = \frac{1}{2} (\Sigma = \pm\frac{1}{2})$ and the term symbol is $^2\Sigma$, a doublet term. The overall parity of the term is added as a right subscript. For H_2^+, the parity of the only occupied orbital is g (Section 11.3c), so the term itself is also g, and in full dress is $^2\Sigma_g$. If there are several electrons, the overall parity is calculated by using

$$g \times g = g \qquad u \times u = g \qquad u \times g = u \qquad (14.1)$$

These rules are generated by interpreting g as $+1$ and u as -1. The term symbol for the ground state of any closed-shell homonuclear diatomic molecule is $^1\Sigma_g$ because the spin is zero (a singlet term in which all electrons paired), there is no orbital angular momentum from a closed shell, and the overall parity is g.

A π electron in a diatomic molecule has one unit of orbital angular momentum about the internuclear axis ($\lambda = \pm 1$), and if it is the only electron outside a closed shell, gives rise to a Π term. If there are two π electrons (as in the ground state of O_2, with configuration $1\pi_u^4 1\pi_g^2$) then the term symbol may be either Σ (if the electrons are travelling in opposite directions, which is the case if they occupy different π orbitals, one with $\lambda = +1$ and the other with $\lambda = -1$) or Δ (if they are travelling in the same direction, which is the case if they occupy the same π orbital, both $\lambda = +1$, for instance). For O_2, the two π electrons occupy different orbitals with parallel spins (a triplet term), so the ground term is $^3\Sigma$. The overall parity of the molecule is

$$(\text{closed shell}) \times g \times g = g$$

The term symbol is therefore $^3\Sigma_g$.

Table 14.2 Properties of O_2 in its lower electronic states*

Configuration†	Term	Relative energy/cm^{-1}	$\tilde{v}$/cm^{-1}	R_e/pm
$\pi_u^2\pi_u^2\pi_g^1\pi_g^1$	$^3\Sigma_g^-$	0	1580	120.74
$\pi_u^2\pi_u^2\pi_g^2\pi_g^0$	$^1\Delta_g$	7 882.39	1509	121.55
$\pi_u^2\pi_u^2\pi_g^1\pi_g^1$	$^1\Sigma_g^+$	13 120.9	1433	122.68
$\pi_u^2\pi_u^1\pi_g^2\pi_g^1$	$^3\Sigma_u^+$	35 713	819	142
$\pi_u^2\pi_u^1\pi_g^2\pi_g^1$	$^3\Sigma_u^-$	49 363	700	160

* Adapted from G. Herzberg, *Spectra of diatomic molecules*, Van Nostrand, New York (1950) and D.C. Harris and M.D. Bertolucci, *Symmetry and spectroscopy: an introduction to vibrational and electronic spectroscopy*, Dover, New York (1989).

† The configuration $\pi_u^2\pi_u^1\pi_g^2\pi_g^1$ should also give rise to a $^3\Delta_u$ term, but electronic transitions to or from this state have not been observed.
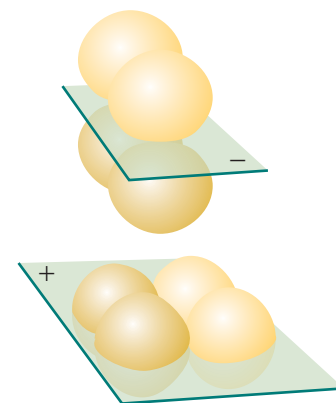

Fig. 14.2 The + or – on a term symbol refers to the overall symmetry of a configuration under reflection in a plane containing the two nuclei.

For Σ terms, a $\pm$ superscript denotes the behaviour of the molecular wavefunction under reflection in a plane containing the nuclei (Fig. 14.2). If, for convenience, we think of O_2 as having one electron in $1\pi_{g,x}$, which changes sign under reflection in the yz-plane, and the other electron in $1\pi_{g,y}$, which does not change sign under reflection in the same plane, then the overall reflection symmetry is

   (closed shell) $\times$ (+) $\times$ (−) = (−)

and the full term symbol of the ground electronic state of O_2 is $^3\Sigma_g^-$.

The term symbols of excited electronic states are constructed in a similar way. For example, the term symbol for the excited state of O_2 formed by placing two electrons in a $1\pi_{g,x}$ (or in a $1\pi_{g,y}$) orbital is $^1\Delta_g$ because $|\Lambda| = 2$ (two electrons in the same π orbital), the spin is zero (all electrons are paired), and the overall parity is (closed shell) $\times$ g $\times$ g = g. Table 14.2 and Fig. 14.3 summarize the configurations, term symbols, and energies of the ground and some excited states of O_2.

(b) Selection rules

A number of selection rules govern which transitions will be observed in the electronic spectrum of a molecule. The selection rules concerned with changes in angular momentum are

   $\Delta\Lambda = 0, \pm1$ $\Delta S = 0$ $\Delta\Sigma = 0$ $\Delta\Omega = 0, \pm1$

where $\Omega = \Lambda + \Sigma$ is the quantum number for the component of total angular momentum (orbital and spin) around the internuclear axis (Fig. 14.4). As in atoms (Section 10.9), the origins of these rules are conservation of angular momentum during a transition and the fact that a photon has a spin of 1.

There are two selection rules concerned with changes in symmetry. First, for Σ terms, only $\Sigma^+ \leftrightarrow \Sigma^+$ and $\Sigma^- \leftrightarrow \Sigma^-$ transitions are allowed. Second, the **Laporte selection rule** for centrosymmetric molecules (those with a centre of inversion) and atoms states that:

   The only allowed transitions are transitions that are accompanied by a change of parity.

That is, u $\rightarrow$ g and g $\rightarrow$ u transitions are allowed, but g $\rightarrow$ g and u $\rightarrow$ u transitions are forbidden.
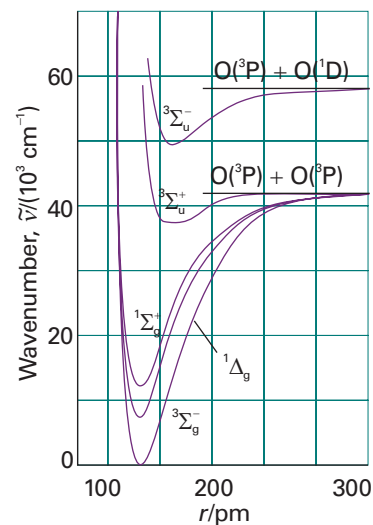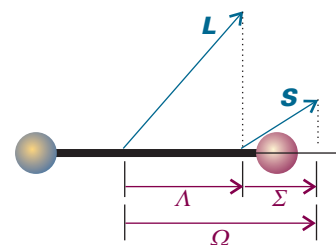

Fig. 14.3 The electronic states of dioxygen.

Fig. 14.4 The coupling of spin and orbital angular momenta in a linear molecule: only the components along the internuclear axis are conserved.
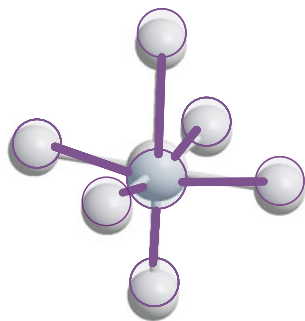
Justification 14.1 *The Laporte selection rule*

The last two selection rules result from the fact that the electric-dipole transition moment

$$\boldsymbol{\mu}_{\mathrm{fi}} = \int \psi_{\mathrm{f}}^{*} \hat{\mu} \, \psi_{\mathrm{i}} \, \mathrm{d}\tau$$

vanishes unless the integrand is invariant under all symmetry operations of the molecule. The three components of the dipole moment operator transform like x, y, and z, and are all u. Therefore, for a g → g transition, the overall parity of the transition dipole moment is g × u × g = u, so it must be zero. Likewise, for a u → u transition, the overall parity is u × u × u = u, so the transition dipole moment must also vanish. Hence, transitions without a change of parity are forbidden. The z-component of the dipole moment operator, the only component of $\boldsymbol{\mu}$ responsible for Σ ↔ Σ transitions, has (+) symmetry. Therefore, for a (+) ↔ (−) transition, the overall symmetry of the transition dipole moment is (+) × (+) × (−) = (−), so it must be zero. Therefore, for Σ terms, $\Sigma^{+} \leftrightarrow \Sigma^{-}$ transitions are not allowed.

Fig. 14.5 A *d–d* transition is parity-forbidden because it corresponds to a g–g transition. However, a vibration of the molecule can destroy the inversion symmetry of the molecule and the g,u classification no longer applies. The removal of the centre of symmetry gives rise to a vibronically allowed transition.

A forbidden g → g transition can become allowed if the centre of symmetry is eliminated by an asymmetrical vibration, such as the one shown in Fig. 14.5. When the centre of symmetry is lost, g → g and u → u transitions are no longer parity-forbidden and become weakly allowed. A transition that derives its intensity from an asymmetrical vibration of a molecule is called a **vibronic transition**.

Self-test 14.1 Which of the following electronic transitions are allowed in O_2: $^{3}\Sigma_{g}^{-} \leftrightarrow {}^{1}\Delta_{g}$, $^{3}\Sigma_{g}^{-} \leftrightarrow {}^{1}\Sigma_{g}^{+}$, $^{3}\Sigma_{g}^{-} \leftrightarrow {}^{3}\Delta_{u}$, $^{3}\Sigma_{g}^{-} \leftrightarrow {}^{3}\Sigma_{u}^{+}$, $^{3}\Sigma_{g}^{-} \leftrightarrow {}^{3}\Sigma_{u}^{-}$? $\qquad [{}^{3}\Sigma_{g}^{-} \leftrightarrow {}^{3}\Sigma_{u}^{-}]$

(c) Vibrational structure

To account for the vibrational structure in electronic spectra of molecules (Fig. 14.6), we apply the **Franck–Condon principle**:

> Because the nuclei are so much more massive than the electrons, an electronic transition takes place very much faster than the nuclei can respond.

As a result of the transition, electron density is rapidly built up in new regions of the molecule and removed from others. The initially stationary nuclei suddenly experience a new force field, to which they respond by beginning to vibrate and (in classical terms) swing backwards and forwards from their original separation (which was maintained during the rapid electronic excitation). The stationary equilibrium separation of the nuclei in the initial electronic state therefore becomes a stationary turning point in the final electronic state (Fig. 14.7).
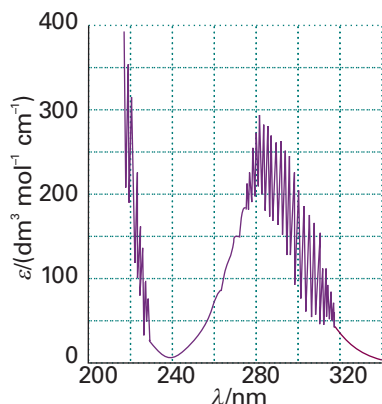

Fig. 14.6 The electronic spectra of some molecules show significant vibrational structure. Shown here is the ultraviolet spectrum of gaseous SO_2 at 298 K. As explained in the text, the sharp lines in this spectrum are due to transitions from a lower electronic state to different vibrational levels of a higher electronic state.

The quantum mechanical version of the Franck–Condon principle refines this picture. Before the absorption, the molecule is in the lowest vibrational state of its lowest electronic state (Fig. 14.8); the most probable location of the nuclei is at their equilibrium separation, R_{e}. The electronic transition is most likely to take place when the nuclei have this separation. When the transition occurs, the molecule is excited to the state represented by the upper curve. According to the Franck–Condon principle, the nuclear framework remains constant during this excitation, so we may imagine the transition as being up the vertical line in Fig. 14.7. The vertical line is the origin of the expression **vertical transition**, which is used to denote an electronic transition that occurs without change of nuclear geometry.

The vertical transition cuts through several vibrational levels of the upper electronic state. The level marked * is the one in which the nuclei are most probably at

the same initial separation R_e (because the vibrational wavefunction has maximum amplitude there), so this vibrational state is the most probable state for the termination of the transition. However, it is not the only accessible vibrational state because several nearby states have an appreciable probability of the nuclei being at the separation R_e. Therefore, transitions occur to all the vibrational states in this region, but most intensely to the state with a vibrational wavefunction that peaks most strongly near R_e.

The vibrational structure of the spectrum depends on the relative horizontal position of the two potential energy curves, and a long **vibrational progression**, a lot of vibrational structure, is stimulated if the upper potential energy curve is appreciably displaced horizontally from the lower. The upper curve is usually displaced to greater equilibrium bond lengths because electronically excited states usually have more antibonding character than electronic ground states.

The separation of the vibrational lines of an electronic absorption spectrum depends on the vibrational energies of the *upper* electronic state. Hence, electronic absorption spectra may be used to assess the force fields and dissociation energies of electronically excited molecules (for example, by using a Birge–Sponer plot, as in Problem 14.2).

(d) Franck–Condon factors

The quantitative form of the Franck–Condon principle is derived from the expression for the transition dipole moment, $\mu_{fi} = \langle f|\mu|i\rangle$. The dipole moment operator is a sum over all nuclei and electrons in the molecule:

$$\hat{\mu} = -e\sum_i r_i + e\sum_I Z_I R_I \tag{14.2}$$

where the vectors are the distances from the centre of charge of the molecule. The intensity of the transition is proportional to the square modulus, $|\mu_{fi}|^2$, of the magnitude of the transition dipole moment (eqn 9.70), and we show in the *Justification* below that this intensity is proportional to the square modulus of the overlap integral, $S(v_f, v_i)$, between the vibrational states of the initial and final electronic states. This overlap integral is a measure of the match between the vibrational wavefunctions in the upper and lower electronic states: $S = 1$ for a perfect match and $S = 0$ when there is no similarity.

....

Justification 14.2 *The Franck–Condon approximation*

The overall state of the molecule consists of an electronic part, $|\varepsilon\rangle$, and a vibrational part, $|v\rangle$. Therefore, within the Born–Oppenheimer approximation, the transition dipole moment factorizes as follows:

$$\mu_{fi} = \langle \varepsilon_f v_f |\{-e\sum_i r_i + e\sum_I Z_I R_I\}| \varepsilon_i v_i\rangle$$

$$= -e\sum_i \langle \varepsilon_f | r_i | \varepsilon_i\rangle\langle v_f | v_i\rangle + e\sum_i Z_i\langle \varepsilon_f | \varepsilon_i\rangle\langle v_f | R_I | v_i\rangle$$

The second term on the right of the second row is zero, because $\langle \varepsilon_f | \varepsilon_i\rangle = 0$ for two different electronic states (they are orthogonal). Therefore,

$$\mu_{fi} = -e\sum_i \langle \varepsilon_f | r_i | \varepsilon_i\rangle\langle v_f | v_i\rangle = \mu_{\varepsilon_f,\varepsilon_i} S(v_f, v_i) \tag{14.3}$$

where

$$\mu_{\varepsilon_f,\varepsilon_i} = -e\sum_i \langle \varepsilon_f | r_i | \varepsilon_i\rangle \quad S(v_f, v_i) = \langle v_f | v_i\rangle \tag{14.4}$$

The matrix element $\mu_{\varepsilon_f,\varepsilon_i}$ is the electric-dipole transition moment arising from the redistribution of electrons (and a measure of the 'kick' this redistribution gives to the electromagnetic field, and vice versa for absorption). The factor $S(v_f, v_i)$, is the overlap integral between the vibrational state $|v_i\rangle$ in the initial electronic state of the molecule, and the vibrational state $|v_f\rangle$ in the final electronic state of the molecule.
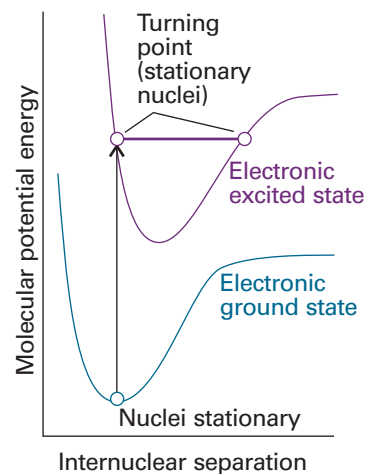
....

Fig. 14.7 According to the Franck–Condon principle, the most intense vibronic transition is from the ground vibrational state to the vibrational state lying vertically above it. Transitions to other vibrational levels also occur, but with lower intensity.
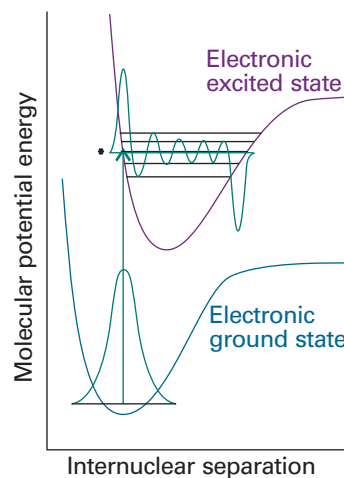

Fig. 14.8 In the quantum mechanical version of the Franck–Condon principle, the molecule undergoes a transition to the upper vibrational state that most closely resembles the vibrational wavefunction of the vibrational ground state of the lower electronic state. The two wavefunctions shown here have the greatest overlap integral of all the vibrational states of the upper electronic state and hence are most closely similar.
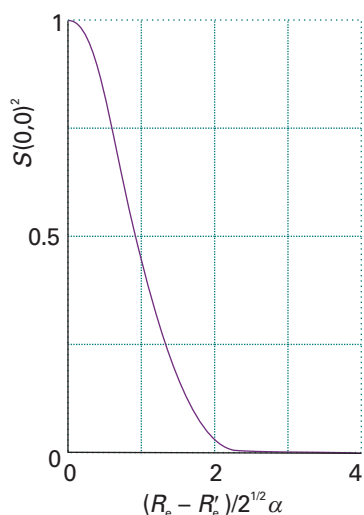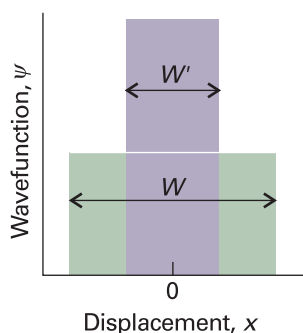
Because the transition intensity is proportional to the square of the magnitude of the transition dipole moment, the intensity of an absorption is proportional to $|S(v_f,v_i)|^2$, which is known as the **Franck–Condon factor** for the transition. It follows that, the greater the overlap of the vibrational state wavefunction in the upper electronic state with the vibrational wavefunction in the lower electronic state, the greater the absorption intensity of that particular simultaneous electronic and vibrational transition. This conclusion is the basis of the illustration in Fig. 14.8, where we see that the vibrational wavefunction of the ground state has the greatest overlap with the vibrational states that have peaks at similar bond lengths in the upper electronic state.

Example 14.1 *Calculating a Franck–Condon factor*

Consider the transition from one electronic state to another, their bond lengths being R_e and R_e' and their force constants equal. Calculate the Franck–Condon factor for the $0-0$ transition and show that the transition is most intense when the bond lengths are equal.

Method We need to calculate $S(0,0)$, the overlap integral of the two ground-state vibrational wavefunctions, and then take its square. The difference between harmonic and anharmonic vibrational wavefunctions is negligible for $v = 0$, so harmonic oscillator wavefunctions can be used (Table 9.1).

Answer We use the (real) wavefunctions

$$\psi_0 = \left(\frac{1}{\alpha\pi^{1/2}}\right)^{1/2} e^{-x^2/2\alpha^2} \qquad \psi_0' = \left(\frac{1}{\alpha\pi^{1/2}}\right)^{1/2} e^{-x'^2/2\alpha^2}$$

where $x = R - R_e$ and $x' = R - R_e'$, with $\alpha = (\hbar^2/mk)^{1/4}$ (Section 9.5a). The overlap integral is

$$S(0,0) = \langle 0|0 \rangle = \int_{-\infty}^{\infty} \psi_0' \psi_0 \, dR = \frac{1}{\alpha\pi^{1/2}} \int_{-\infty}^{\infty} e^{-(x^2+x'^2)/2\alpha^2} dx$$

We now write $\alpha z = R - \frac{1}{2}(R_e + R_e')$, and manipulate this expression into

$$S(0,0) = \frac{1}{\pi^{1/2}} e^{-(R_e-R_e')^2/4\alpha^2} \int_{-\infty}^{\infty} e^{-z^2} dz$$

The value of the integral is $\pi^{1/2}$. Therefore, the overlap integral is

$$S(0,0) = e^{-(R_e-R_e')^2/4\alpha^2}$$

and the Franck–Condon factor is

$$S(0,0)^2 = e^{-(R_e-R_e')^2/2\alpha^2}$$

This factor is equal to 1 when $R_e' = R_e$ and decreases as the equilibrium bond lengths diverge from each other (Fig. 14.9).

For Br_2, $R_e = 228$ pm and there is an upper state with $R_e' = 266$ pm. Taking the vibrational wavenumber as 250 cm^{-1} gives $S(0,0)^2 = 5.1 \times 10^{-10}$, so the intensity of the $0-0$ transition is only 5.1×10^{-10} what it would have been if the potential curves had been directly above each other.

Self-test 14.2 Suppose the vibrational wavefunctions can be approximated by rectangular functions of width W and W', centred on the equilibrium bond lengths (Fig. 14.10). Find the corresponding Franck–Condon factors when the centres are coincident and $W' < W$. $[S^2 = W'/W]$

Fig. 14.9 The Franck–Condon factor for the arrangement discussed in Example 14.1.

Fig. 14.10 The model wavefunctions used in Self-test 14.2.

(e) Rotational structure

Just as in vibrational spectroscopy, where a vibrational transition is accompanied by rotational excitation, so rotational transitions accompany the excitation of the vibrational excitation that accompanies electronic excitation. We therefore see P, Q, and R branches for each vibrational transition, and the electronic transition has a very rich structure. However, the principal difference is that electronic excitation can result in much larger changes in bond length than vibrational excitation causes alone, and the rotational branches have a more complex structure than in vibration–rotation spectra.

We suppose that the rotational constants of the electronic ground and excited states are B and B', respectively. The rotational energy levels of the initial and final states are

$$E(J) = hcBJ(J+1) \qquad E(J') = hcB'J'(J'+1)$$

and the rotational transitions occur at the following positions relative to the vibrational transition of wavenumber $\tilde{v}$ that they accompany:

P branch ($\Delta J = -1$): $\qquad \tilde{v}_P(J) = \tilde{v} - (B'+B)J + (B'-B)J^2$ (14.5a)

Q branch ($\Delta J = 0$): $\qquad \tilde{v}_Q(J) = \tilde{v} + (B'-B)J(J+1)$ (14.5b)

R branch ($\Delta J = +1$): $\qquad \tilde{v}_R(J) = \tilde{v} + (B'+B)(J+1) + (B'-B)(J+1)^2$ (14.5c)

(These are the analogues of eqn 13.63.) First, suppose that the bond length in the electronically excited state is greater than that in the ground state; then $B' < B$ and $B' - B$ is negative. In this case the lines of the R branch converge with increasing J and when J is such that $|B' - B|(J+1) > B' + B$ the lines start to appear at successively decreasing wavenumbers. That is, the R branch has a **band head** (Fig. 14.11a). When the bond is shorter in the excited state than in the ground state, $B' > B$ and $B' - B$ is positive. In this case, the lines of the P branch begin to converge and go through a head when J is such that $(B' - B)J > B' + B$ (Fig. 14.11b).
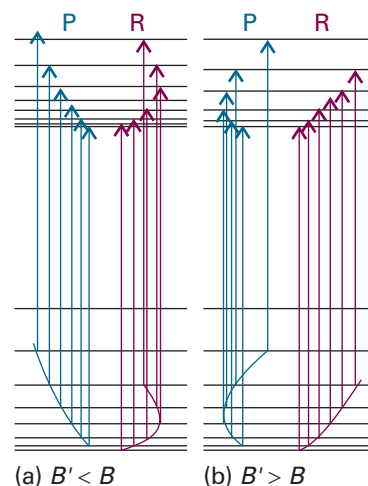
14.2 The electronic spectra of polyatomic molecules

The absorption of a photon can often be traced to the excitation of specific types of electrons or to electrons that belong to a small group of atoms in a polyatomic molecule. For example, when a carbonyl group ($>C=O$) is present, an absorption at about 290 nm is normally observed, although its precise location depends on the nature of the rest of the molecule. Groups with characteristic optical absorptions are called **chromophores** (from the Greek for 'colour bringer'), and their presence often accounts for the colours of substances (Table 14.3).

(a) d–d transitions

In a free atom, all five d orbitals of a given shell are degenerate. In a d-metal complex, where the immediate environment of the atom is no longer spherical, the d orbitals

Fig. 14.11 When the rotational constants of a diatomic molecule differ significantly in the initial and final states of an electronic transition, the P and R branches show a head. (a) The formation of a head in the R branch when $B' < B$; (b) the formation of a head in the P branch when $B' > B$.

Comment 14.2
The web site for this text contains links to databases of electronic spectra.

Synoptic table 14.3* Absorption characteristics of some groups and molecules

Group	$\tilde{v}/\text{cm}^{-1}$	λ_{max}/nm	$\varepsilon/(\text{dm}^3\,\text{mol}^{-1}\,\text{cm}^{-1})$
$C=C$ ($\pi^* \leftarrow \pi$)	61 000	163	5 000
	57 300	174	15 500
$C=O$ ($\pi^* \leftarrow n$)	35 000–37 000	270–290	10–20
H_2O ($\pi^* \leftarrow n$)	60 000	167	7 000

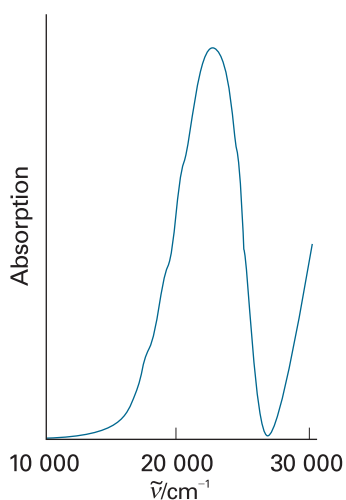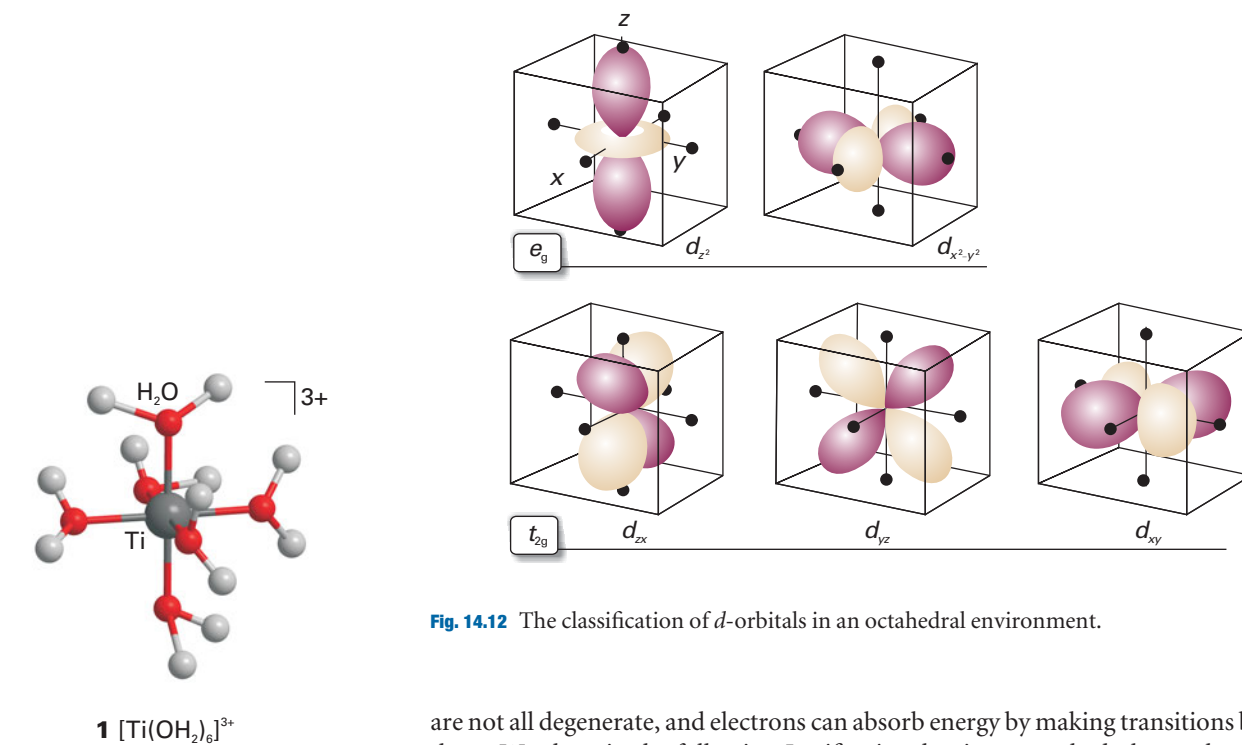* More values are given in the *Data section*.

Fig. 14.12 The classification of *d*-orbitals in an octahedral environment.

1 $[Ti(OH_2)_6]^{3+}$

2

Fig. 14.13 The electronic absorption spectrum of $[Ti(OH_2)_6]^{3+}$ in aqueous solution.

are not all degenerate, and electrons can absorb energy by making transitions between them. We show in the following *Justification* that in an octahedral complex, such as $[Ti(OH_2)_6]^{3+}$ (**1**), the five *d* orbitals of the central atom are split into two sets (**2**), a triply degenerate set labelled t_{2g} and a doubly degenerate set labelled e_g. The three t_{2g} orbitals lie below the two e_g orbitals; the difference in energy is denoted Δ_O and called the **ligand-field splitting parameter** (the O denoting octahedral symmetry).

....

Justification 14.3 *The splitting of* d-*orbitals in an octahedral* d-*metal complex*

In an octahedral *d*-metal complex, six identical ions or molecules, the *ligands*, are at the vertices of a regular octahedron, with the metal ion at its centre. The ligands can be regarded as point negative charges that are repelled by the *d*-electrons of the central ion. Figure 14.12 shows the consequence of this arrangement: the five *d*-orbitals fall into two groups, with $d_{x^2-y^2}$ and d_{z^2} pointing directly towards the ligand positions, and d_{xy}, d_{yz}, and d_{zx} pointing between them. An electron occupying an orbital of the former group has a less favourable potential energy than when it occupies any of the three orbitals of the other group, and so the *d*-orbitals split into the two sets shown in (**2**) with an energy difference Δ_O: a triply degenerate set comprising the d_{xy}, d_{yz}, and d_{zx} orbitals and labelled t_{2g}, and a doubly degenerate set comprising the $d_{x^2-y^2}$ and d_{z^2} orbitals and labelled e_g.

....

The *d*-orbitals also divide into two sets in a tetrahedral complex, but in this case the *e* orbitals lie below the t_2 orbitals and their separation is written Δ_T. Neither Δ_O nor Δ_T is large, so transitions between the two sets of orbitals typically occur in the visible region of the spectrum. The transitions are responsible for many of the colours that are so characteristic of *d*-metal complexes. As an example, the spectrum of $[Ti(OH_2)_6]^{3+}$ near 20 000 cm^{-1} (500 nm) is shown in Fig. 14.13, and can be ascribed to the promotion of its single *d* electron from a t_{2g} orbital to an e_g orbital. The wavenumber of the absorption maximum suggests that $\Delta_O \approx 20\ 000$ cm^{-1} for this complex, which corresponds to about 2.5 eV.

According to the Laporte rule (Section 14.1b), d–d transitions are parity-forbidden in octahedral complexes because they are g → g transitions (more specifically $e_g \leftarrow t_{2g}$ transitions). However, d–d transitions become weakly allowed as vibronic transitions as a result of coupling to asymmetrical vibrations such as that shown in Fig. 14.5.

(b) Charge-transfer transitions

A complex may absorb radiation as a result of the transfer of an electron from the ligands into the d-orbitals of the central atom, or vice versa. In such **charge-transfer transitions** the electron moves through a considerable distance, which means that the transition dipole moment may be large and the absorption is correspondingly intense. This mode of chromophore activity is shown by the permanganate ion, MnO_4^-, and accounts for its intense violet colour (which arises from strong absorption within the range 420–700 nm). In this oxoanion, the electron migrates from an orbital that is largely confined to the O atom ligands to an orbital that is largely confined to the Mn atom. It is therefore an example of a **ligand-to-metal charge-transfer transition** (LMCT). The reverse migration, a **metal-to-ligand charge-transfer transition** (MLCT), can also occur. An example is the transfer of a d electron into the antibonding π orbitals of an aromatic ligand. The resulting excited state may have a very long lifetime if the electron is extensively delocalized over several aromatic rings, and such species can participate in photochemically induced redox reactions (see Section 23.7).

The intensities of charge-transfer transitions are proportional to the square of the transition dipole moment, in the usual way. We can think of the transition moment as a measure of the distance moved by the electron as it migrates from metal to ligand or vice versa, with a large distance of migration corresponding to a large transition dipole moment and therefore a high intensity of absorption. However, because the integrand in the transition dipole is proportional to the product of the initial and final wavefunctions, it is zero unless the two wavefunctions have nonzero values in the same region of space. Therefore, although large distances of migration favour high intensities, the diminished overlap of the initial and final wavefunctions for large separations of metal and ligands favours low intensities (see Problem 14.17). We encounter similar considerations when we examine electron transfer reactions (Chapter 24), which can be regarded as a special type of charge-transfer transition.

(c) $\pi^* \leftarrow \pi$ and $\pi^* \leftarrow n$ transitions

Absorption by a C=C double bond results in the excitation of a π electron into an antibonding π^* orbital (Fig. 14.14). The chromophore activity is therefore due to a $\pi^* \leftarrow \pi$ transition (which is normally read 'π to π-star transition'). Its energy is about 7 eV for an unconjugated double bond, which corresponds to an absorption at 180 nm (in the ultraviolet). When the double bond is part of a conjugated chain, the energies of the molecular orbitals lie closer together and the $\pi^* \leftarrow \pi$ transition moves to longer wavelength; it may even lie in the visible region if the conjugated system is long enough. An important example of an $\pi^* \leftarrow \pi$ transition is provided by the photochemical mechanism of vision (*Impact I14.1*).

The transition responsible for absorption in carbonyl compounds can be traced to the lone pairs of electrons on the O atom. The Lewis concept of a 'lone pair' of electrons is represented in molecular orbital theory by a pair of electrons in an orbital confined largely to one atom and not appreciably involved in bond formation. One of these electrons may be excited into an empty π^* orbital of the carbonyl group (Fig. 14.15), which gives rise to a $\pi^* \leftarrow n$ transition (an 'n to π-star transition'). Typical absorption energies are about 4 eV (290 nm). Because $\pi^* \leftarrow n$ transitions in carbonyls are symmetry forbidden, the absorptions are weak.
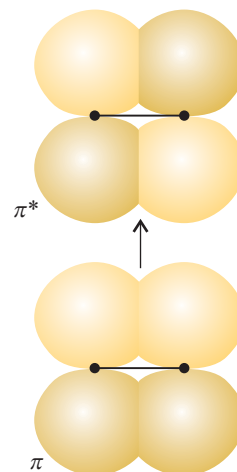

Fig. 14.14 A C=C double bond acts as a chromophore. One of its important transitions is the $\pi^* \leftarrow \pi$ transition illustrated here, in which an electron is promoted from a π orbital to the corresponding antibonding orbital.
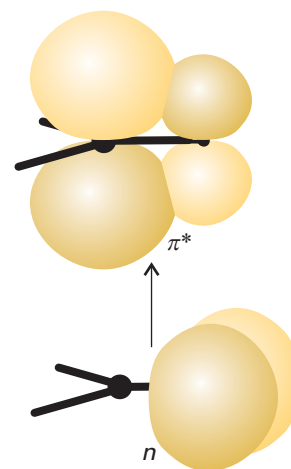

Fig. 14.15 A carbonyl group (C=O) acts as a chromophore primarily on account of the excitation of a nonbonding O lone-pair electron to an antibonding CO π orbital.
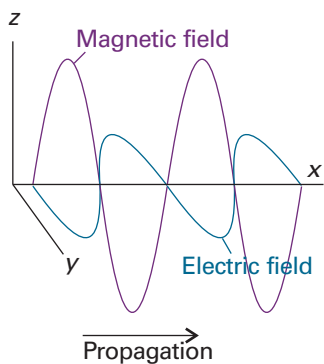
Fig. 14.16 Electromagnetic radiation consists of a wave of electric and magnetic fields perpendicular to the direction of propagation (in this case the *x*-direction), and mutually perpendicular to each other. This illustration shows a plane-polarized wave, with the electric and magnetic fields oscillating in the *xy* and *xz* planes, respectively.

(d) Circular dichroism spectroscopy

Electronic spectra can reveal additional details of molecular structure when experiments are conducted with **polarized light**, electromagnetic radiation with electric and magnetic fields that oscillate only in certain directions. Light is **plane polarized** when the electric and magnetic fields each oscillate in a single plane (Fig. 14.16). The plane of polarization may be oriented in any direction around the direction of propagation (the *x*-direction in Fig. 14.16), with the electric and magnetic fields perpendicular to that direction (and perpendicular to each other). An alternative mode of polarization is **circular polarization**, in which the electric and magnetic fields rotate around the direction of propagation in either a clockwise or a counter-clockwise sense but remain perpendicular to it and each other.

When plane-polarized radiation passes through samples of certain kinds of matter, the plane of polarization is rotated around the direction of propagation. This rotation is the familiar phenomenon of optical activity, observed when the molecules in the sample are chiral (Section 12.3b). Chiral molecules have a second characteristic: they absorb left and right circularly polarized light to different extents. In a circularly polarized ray of light, the electric field describes a helical path as the wave travels through space (Fig. 14.17), and the rotation may be either clockwise or counterclockwise. The differential absorption of left- and right-circularly polarized light is called **circular dichroism**. In terms of the absorbances for the two components, A_L and A_R, the circular dichroism of a sample of molar concentration [J] is reported as

$$\Delta\varepsilon = \varepsilon_L - \varepsilon_R = \frac{A_L - A_R}{[J]l} \tag{14.6}$$

where *l* is the path length of the sample.

Circular dichroism is a useful adjunct to visible and UV spectroscopy. For example, the CD spectra of the enantiomeric pairs of chiral *d*-metal complexes are distinctly different, whereas there is little difference between their absorption spectra (Fig. 14.18). Moreover, CD spectra can be used to assign the absolute configuration of complexes by comparing the observed spectrum with the CD spectrum of a similar complex of known handedness. We shall see in Chapter 19 that the CD spectra of biological polymers, such as proteins and nucleic acids, give similar structural information. In these cases the spectrum of the polymer chain arises from the chirality of individual monomer units and, in addition, a contribution from the three-dimensional structure of the polymer itself.
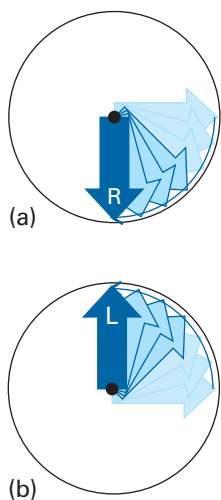

Fig. 14.17 In circularly polarized light, the electric field at different points along the direction of propagation rotates. The arrays of arrows in these illustrations show the view of the electric field when looking toward the oncoming ray: (a) right-circularly polarized, (b) left-circularly polarized light.

IMPACT ON BIOCHEMISTRY
I14.1 Vision

The eye is an exquisite photochemical organ that acts as a transducer, converting radiant energy into electrical signals that travel along neurons. Here we concentrate on the events taking place in the human eye, but similar processes occur in all animals. Indeed, a single type of protein, rhodopsin, is the primary receptor for light throughout the animal kingdom, which indicates that vision emerged very early in evolutionary history, no doubt because of its enormous value for survival.

Photons enter the eye through the cornea, pass through the ocular fluid that fills the eye, and fall on the retina. The ocular fluid is principally water, and passage of light through this medium is largely responsible for the *chromatic aberration* of the eye, the blurring of the image as a result of different frequencies being brought to slightly different focuses. The chromatic aberration is reduced to some extent by the tinted region called the *macular pigment* that covers part of the retina. The pigments in this region are the carotene-like xanthophylls (**3**), which absorb some of the blue light and
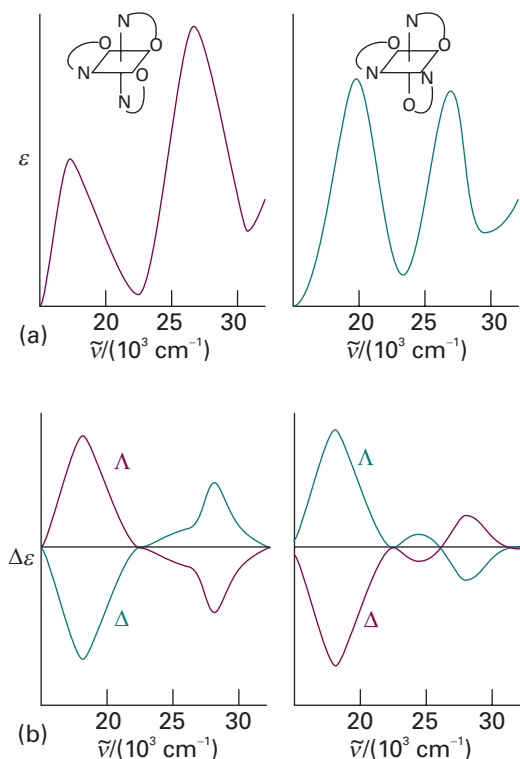
Fig. 14.18 (a) The absorption spectra of two isomers, denoted mer and fac, of [Co(ala)$_3$], where ala is the conjugate base of alanine, and (b) the corresponding CD spectra. The left- and right-handed forms of these isomers give identical absorption spectra. However, the CD spectra are distinctly different, and the absolute configurations (denoted Λ and Δ) have been assigned by comparison with the CD spectra of a complex of known absolute configuration.
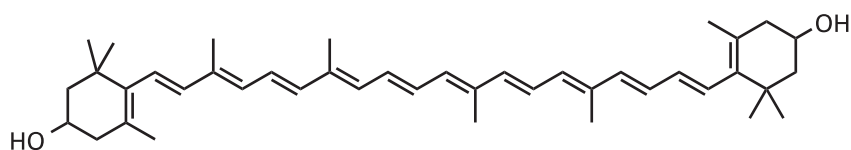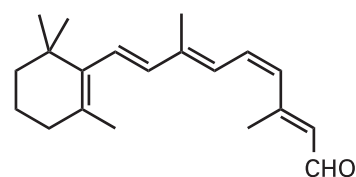

3 A xanthophyll

hence help to sharpen the image. They also protect the photoreceptor molecules from too great a flux of potentially dangerous high energy photons. The xanthophylls have delocalized electrons that spread along the chain of conjugated double bonds, and the $\pi^\star \leftarrow \pi$ transition lies in the visible.

About 57 per cent of the photons that enter the eye reach the retina; the rest are scattered or absorbed by the ocular fluid. Here the primary act of vision takes place, in which the chromophore of a rhodopsin molecule absorbs a photon in another $\pi^\star \leftarrow \pi$ transition. A rhodopsin molecule consists of an opsin protein molecule to which is attached a 11-*cis*-retinal molecule (**4**). The latter resembles half a carotene molecule, showing Nature's economy in its use of available materials. The attachment is by the formation of a protonated Schiff's base, utilizing the —CHO group of the chromophore and the terminal NH$_2$ group of the sidechain, a lysine residue from opsin. The free 11-*cis*-retinal molecule absorbs in the ultraviolet, but attachment to the opsin protein molecule shifts the absorption into the visible region. The rhodopsin molecules are situated in the membranes of special cells (the 'rods' and the 'cones') that cover the retina. The opsin molecule is anchored into the cell membrane by two hydrophobic groups and largely surrounds the chromophore (Fig. 14.19).

Immediately after the absorption of a photon, the 11-*cis*-retinal molecule undergoes photoisomerization into all-*trans*-retinal (**5**). Photoisomerization takes about

4 11-*cis*-retinal

Fig. 14.19 The structure of the rhodopsin molecule, consisting of an opsin protein to which is attached an 11-*cis*-retinal molecule embedded in the space surrounded by the helical regions.
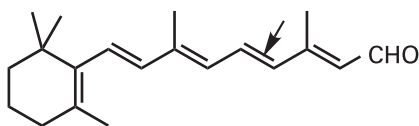
5 All-*trans*-retinal

200 fs and about 67 pigment molecules isomerize for every 100 photons that are absorbed. The process occurs because the $\pi^\star \leftarrow \pi$ excitation of an electron loosens one of the π-bonds (the one indicated by the arrow in **5**), its torsional rigidity is lost, and one part of the molecule swings round into its new position. At that point, the molecule returns to its ground state, but is now trapped in its new conformation. The straightened tail of all-*trans*-retinal results in the molecule taking up more space than 11-*cis*-retinal did, so the molecule presses against the coils of the opsin molecule that surrounds it. In about 0.25–0.50 ms from the initial absorption event, the rhodopsin molecule is activated both by the isomerization of retinal and deprotonation of its Schiff's base tether to opsin, forming an intermediate known as *metarhodopsin II*.

In a sequence of biochemical events known as the *biochemical cascade*, metarhodopsin II activates the protein transducin, which in turn activates a phosphodiesterase enzyme that hydrolyses cyclic guanine monophosphate (cGMP) to GMP. The reduction in the concentration of cGMP causes ion channels, proteins that mediate the movement of ions across biological membranes, to close and the result is a sizable change in the transmembrane potential (see *Impact I7.2* for a discussion of transmembrane potentials). The pulse of electric potential travels through the optical nerve and into the optical cortex, where it is interpreted as a signal and incorporated into the web of events we call 'vision'.

The resting state of the rhodopsin molecule is restored by a series of nonradiative chemical events powered by ATP. The process involves the escape of all-*trans*-retinal as all-*trans*-retinol (in which —CHO has been reduced to —CH$_2$OH) from the opsin molecule by a process catalysed by the enzyme rhodopsin kinase and the attachment of another protein molecule, arrestin. The free all-*trans*-retinol molecule now undergoes enzyme-catalysed isomerization into 11-*cis*-retinol followed by dehydrogenation to form 11-*cis*-retinal, which is then delivered back into an opsin molecule. At this point, the cycle of excitation, photoisomerization, and regeneration is ready to begin again.

The fates of electronically excited states

A **radiative decay process** is a process in which a molecule discards its excitation energy as a photon. A more common fate is **nonradiative decay**, in which the excess energy is transferred into the vibration, rotation, and translation of the surrounding molecules. This thermal degradation converts the excitation energy completely into thermal motion of the environment (that is, to 'heat'). An excited molecule may also take part in a chemical reaction, as we discuss in Chapter 23.

14.3 Fluorescence and phosphorescence

In **fluorescence**, spontaneous emission of radiation occurs within a few nanoseconds after the exciting radiation is extinguished (Fig. 14.20). In **phosphorescence**, the spontaneous emission may persist for long periods (even hours, but characteristically seconds or fractions of seconds). The difference suggests that fluorescence is a fast conversion of absorbed radiation into re-emitted energy, and that phosphorescence involves the storage of energy in a reservoir from which it slowly leaks.

(a) Fluorescence

Figure 14.21 shows the sequence of steps involved in fluorescence. The initial absorption takes the molecule to an excited electronic state, and if the absorption spectrum were monitored it would look like the one shown in Fig. 14.22a. The excited molecule
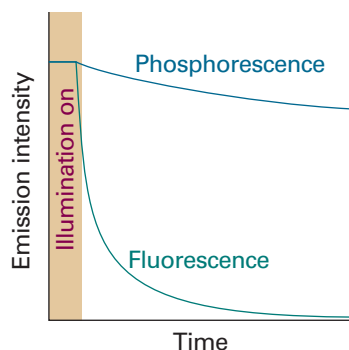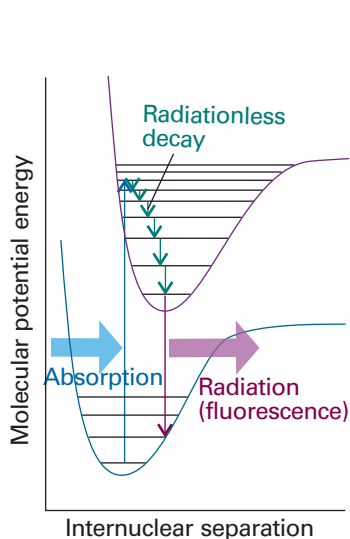

Fig. 14.20 The empirical (observation-based) distinction between fluorescence and phosphorescence is that the former is extinguished very quickly after the exciting source is removed, whereas the latter continues with relatively slowly diminishing intensity.

Fig. 14.21 The sequence of steps leading to fluorescence. After the initial absorption, the upper vibrational states undergo radiationless decay by giving up energy to the surroundings. A radiative transition then occurs from the vibrational ground state of the upper electronic state.
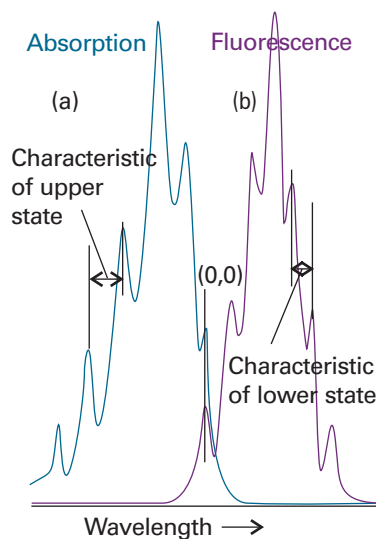
Fig. 14.22 An absorption spectrum (a) shows a vibrational structure characteristic of the upper state. A fluorescence spectrum (b) shows a structure characteristic of the lower state; it is also displaced to lower frequencies (but the 0–0 transitions are coincident) and resembles a mirror image of the absorption.

is subjected to collisions with the surrounding molecules, and as it gives up energy nonradiatively it steps down the ladder of vibrational levels to the lowest vibrational level of the electronically excited molecular state. The surrounding molecules, however, might now be unable to accept the larger energy difference needed to lower the molecule to the ground electronic state. It might therefore survive long enough to undergo spontaneous emission, and emit the remaining excess energy as radiation. The downward electronic transition is vertical (in accord with the Franck–Condon principle) and the fluorescence spectrum has a vibrational structure characteristic of the *lower* electronic state (Fig. 14.22b).

Provided they can be seen, the 0–0 absorption and fluorescence transitions can be expected to be coincident. The absorption spectrum arises from 1–0, 2–0, . . . transitions that occur at progressively higher wavenumber and with intensities governed by the Franck–Condon principle. The fluorescence spectrum arises from 0–0, 0–1, . . . *downward* transitions that hence occur with decreasing wavenumbers. The 0–0 absorption and fluorescence peaks are not always exactly coincident, however, because the solvent may interact differently with the solute in the ground and excited states (for instance, the hydrogen bonding pattern might differ). Because the solvent molecules do not have time to rearrange during the transition, the absorption occurs in an environment characteristic of the solvated ground state; however, the fluorescence occurs in an environment characteristic of the solvated excited state (Fig. 14.23).

Fluorescence occurs at lower frequencies (longer wavelengths) than the incident radiation because the emissive transition occurs after some vibrational energy has been discarded into the surroundings. The vivid oranges and greens of fluorescent dyes are an everyday manifestation of this effect: they absorb in the ultraviolet and blue, and fluoresce in the visible. The mechanism also suggests that the intensity of the fluorescence ought to depend on the ability of the solvent molecules to accept the
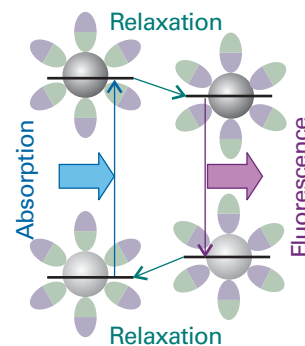

Fig. 14.23 The solvent can shift the fluorescence spectrum relative to the absorption spectrum. On the left we see that the absorption occurs with the solvent (the ellipses) in the arrangement characteristic of the ground electronic state of the molecule (the sphere). However, before fluorescence occurs, the solvent molecules relax into a new arrangement, and that arrangement is preserved during the subsequent radiative transition.
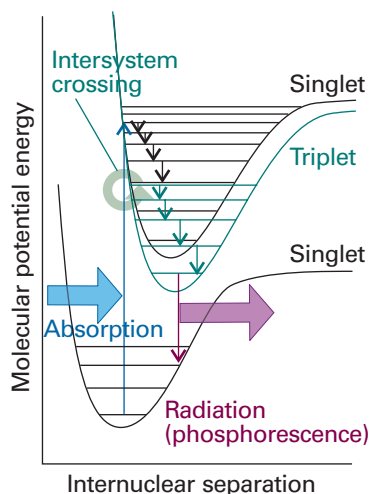
electronic and vibrational quanta. It is indeed found that a solvent composed of molecules with widely spaced vibrational levels (such as water) can in some cases accept the large quantum of electronic energy and so extinguish, or 'quench', the fluorescence. We examine the mechanisms of fluorescence quenching in Chapter 23.

(b) Phosphorescence

Figure 14.24 shows the sequence of events leading to phosphorescence for a molecule with a singlet ground state. The first steps are the same as in fluorescence, but the presence of a triplet excited state plays a decisive role. The singlet and triplet excited states share a common geometry at the point where their potential energy curves intersect. Hence, if there is a mechanism for unpairing two electron spins (and achieving the conversion of $\uparrow\downarrow$ to $\uparrow\uparrow$), the molecule may undergo **intersystem crossing**, a nonradiative transition between states of different multiplicity, and become a triplet state. We saw in the discussion of atomic spectra (Section 10.9d) that singlet–triplet transitions may occur in the presence of spin–orbit coupling, and the same is true in molecules. We can expect intersystem crossing to be important when a molecule contains a moderately heavy atom (such as S), because then the spin–orbit coupling is large.

If an excited molecule crosses into a triplet state, it continues to deposit energy into the surroundings. However, it is now stepping down the triplet's vibrational ladder, and at the lowest energy level it is trapped because the triplet state is at a lower energy than the corresponding singlet (recall Hund's rule, Section 13.7). The solvent cannot absorb the final, large quantum of electronic excitation energy, and the molecule cannot radiate its energy because return to the ground state is spin-forbidden (Section 14.1). The radiative transition, however, is not totally forbidden because the spin–orbit coupling that was responsible for the intersystem crossing also breaks the selection rule. The molecules are therefore able to emit weakly, and the emission may continue long after the original excited state was formed.

The mechanism accounts for the observation that the excitation energy seems to get trapped in a slowly leaking reservoir. It also suggests (as is confirmed experimentally) that phosphorescence should be most intense from solid samples: energy transfer is then less efficient and intersystem crossing has time to occur as the singlet excited state steps slowly past the intersection point. The mechanism also suggests that the phosphorescence efficiency should depend on the presence of a moderately heavy atom (with strong spin–orbit coupling), which is in fact the case. The confirmation of the mechanism is the experimental observation (using the sensitive magnetic resonance techniques described in Chapter 15) that the sample is paramagnetic while the reservoir state, with its unpaired electron spins, is populated.

The various types of nonradiative and radiative transitions that can occur in molecules are often represented on a schematic **Jablonski diagram** of the type shown in Fig. 14.25.

Fig. 14.24 The sequence of steps leading to phosphorescence. The important step is the intersystem crossing, the switch from a singlet state to a triplet state brought about by spin–orbit coupling. The triplet state acts as a slowly radiating reservoir because the return to the ground state is spin-forbidden.
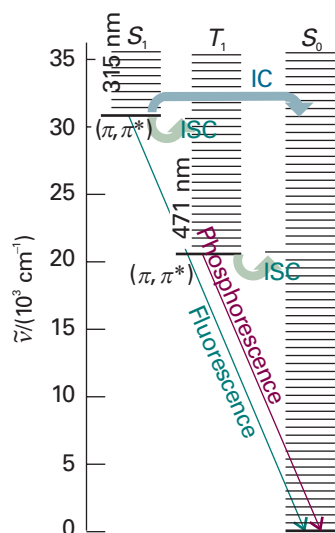

Fig. 14.25 A Jablonski diagram (here, for naphthalene) is a simplified portrayal of the relative positions of the electronic energy levels of a molecule. Vibrational levels of states of a given electronic state lie above each other, but the relative horizontal locations of the columns bear no relation to the nuclear separations in the states. The ground vibrational states of each electronic state are correctly located vertically but the other vibrational states are shown only schematically. (IC: internal conversion; ISC: intersystem crossing.)

IMPACT ON BIOCHEMISTRY
### I14.2 Fluorescence microscopy

Apart from a small number of co-factors, such as the chlorophylls and flavins, the majority of the building blocks of proteins and nucleic acids do not fluoresce strongly. Four notable exceptions are the amino acids tryptophan ($\lambda_{abs} \approx 280$ nm and $\lambda_{fluor} \approx 348$ nm in water), tyrosine ($\lambda_{abs} \approx 274$ nm and $\lambda_{fluor} \approx 303$ nm in water), and phenylalanine ($\lambda_{abs} \approx 257$ nm and $\lambda_{fluor} \approx 282$ nm in water), and the oxidized form of the sequence serine–tyrosine–glycine (**6**) found in the green fluorescent protein (GFP) of certain jellyfish. The wild type of GFP from *Aequora victoria* absorbs strongly at 395 nm and emits maximally at 509 nm.

In **fluorescence microscopy**, images of biological cells at work are obtained by attaching a large number of fluorescent molecules to proteins, nucleic acids, and membranes and then measuring the distribution of fluorescence intensity within the illuminated area. A common fluorescent label is GFP. With proper filtering to remove light due to Rayleigh scattering of the incident beam, it is possible to collect light from the sample that contains only fluorescence from the label. However, great care is required to eliminate fluorescent impurities from the sample.

14.4 Dissociation and predissociation

Another fate for an electronically excited molecule is **dissociation**, the breaking of bonds (Fig. 14.26). The onset of dissociation can be detected in an absorption spectrum by seeing that the vibrational structure of a band terminates at a certain energy. Absorption occurs in a continuous band above this **dissociation limit** because the final state is an unquantized translational motion of the fragments. Locating the dissociation limit is a valuable way of determining the bond dissociation energy.

In some cases, the vibrational structure disappears but resumes at higher photon energies. This **predissociation** can be interpreted in terms of the molecular potential energy curves shown in Fig. 14.27. When a molecule is excited to a vibrational level, its electrons may undergo a redistribution that results in it undergoing an **internal conversion**, a radiationless conversion to another state of the same multiplicity. An internal conversion occurs most readily at the point of intersection of the two molecular potential energy curves, because there the nuclear geometries of the two states are the same. The state into which the molecule converts may be dissociative, so the states near the intersection have a finite lifetime, and hence their energies are imprecisely defined. As a result, the absorption spectrum is blurred in the vicinity of the intersection. When the incoming photon brings enough energy to excite the molecule
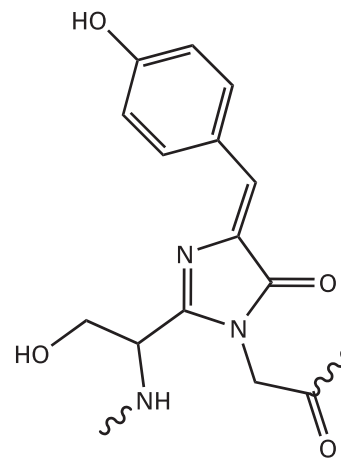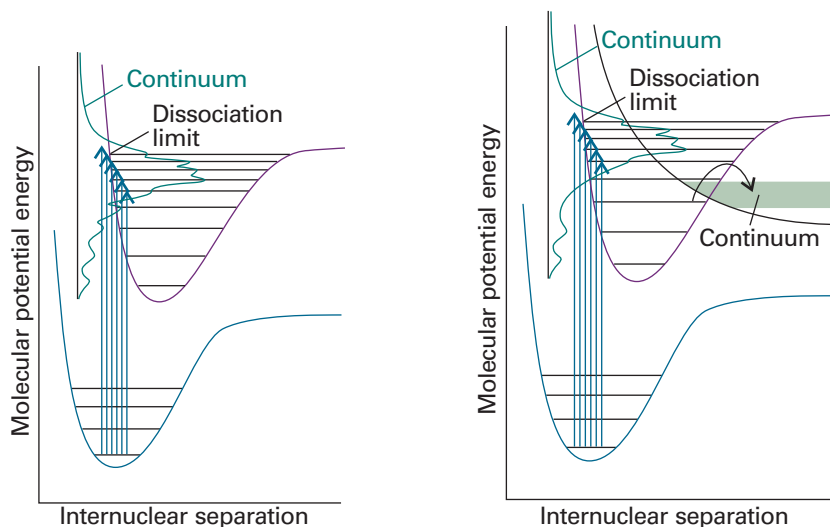
6 The chromophore of GFP

Fig. 14.26 When absorption occurs to unbound states of the upper electronic state, the molecule dissociates and the absorption is a continuum. Below the dissociation limit the electronic spectrum shows a normal vibrational structure.

Fig. 14.27 When a dissociative state crosses a bound state, as in the upper part of the illustration, molecules excited to levels near the crossing may dissociate. This process is called predissociation, and is detected in the spectrum as a loss of vibrational structure that resumes at higher frequencies.

to a vibrational level high above the intersection, the internal conversion does not occur (the nuclei are unlikely to have the same geometry). Consequently, the levels resume their well-defined, vibrational character with correspondingly well-defined energies, and the line structure resumes on the high-frequency side of the blurred region.

Lasers

Lasers have transformed chemistry as much as they have transformed the everyday world. They lie very much on the frontier of physics and chemistry, for their operation depends on details of optics and, in some cases, of solid-state processes. In this section, we discuss the mechanisms of laser action, and then explore their applications in chemistry. In *Further information 14.1*, we discuss the modes of operation of a number of commonly available laser systems.

14.5 General principles of laser action

The word laser is an acronym formed from **l**ight **a**mplification by **s**timulated **e**mission of **r**adiation. In stimulated emission, an excited state is stimulated to emit a photon by radiation of the same frequency; the more photons that are present, the greater the probability of the emission. The essential feature of laser action is positive-feedback: the more photons present of the appropriate frequency, the more photons of that frequency that will be stimulated to form.
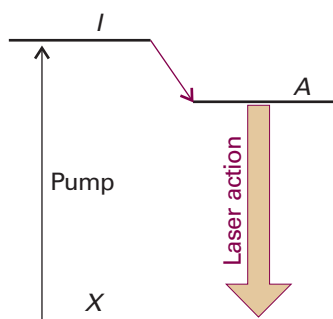
(a) Population inversion

Fig. 14.28 The transitions involved in one kind of three-level laser. The pumping pulse populates the intermediate state I, which in turn populates the laser state A. The laser transition is the stimulated emission $A \rightarrow X$.

One requirement of laser action is the existence of a **metastable excited state**, an excited state with a long enough lifetime for it to participate in stimulated emission. Another requirement is the existence of a greater population in the metastable state than in the lower state where the transition terminates, for then there will be a net emission of radiation. Because at thermal equilibrium the opposite is true, it is necessary to achieve a **population inversion** in which there are more molecules in the upper state than in the lower.

One way of achieving population inversion is illustrated in Fig. 14.28. The molecule is excited to an intermediate state I, which then gives up some of its energy nonradiatively and changes into a lower state A; the laser transition is the return of A to the ground state X. Because three energy levels are involved overall, this arrangement leads to a **three-level laser**. In practice, I consists of many states, all of which can convert to the upper of the two laser states A. The $I \leftarrow X$ transition is stimulated with an intense flash of light in the process called **pumping**. The pumping is often achieved with an electric discharge through xenon or with the light of another laser. The conversion of I to A should be rapid, and the laser transitions from A to X should be relatively slow.

The disadvantage of this three-level arrangement is that it is difficult to achieve population inversion, because so many ground-state molecules must be converted to the excited state by the pumping action. The arrangement adopted in a **four-level laser** simplifies this task by having the laser transition terminate in a state A' other than the ground state (Fig. 14.29). Because A' is unpopulated initially, any population in A corresponds to a population inversion, and we can expect laser action if A is sufficiently metastable. Moreover, this population inversion can be maintained if the $A' \leftarrow X$ transitions are rapid, for these transitions will deplete any population in A' that stems from the laser transition, and keep the state A' relatively empty.
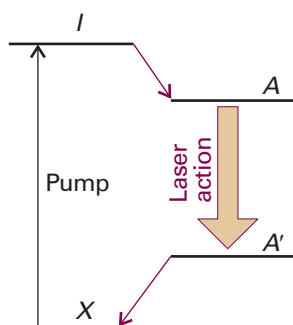
Fig. 14.29 The transitions involved in a four-level laser. Because the laser transition terminates in an excited state (A'), the population inversion between A and A' is much easier to achieve.